

A New Perspective on Scale Uncertainties for Diboson Processes

Prerit Jaiswal

*Department of Physics, Florida State University,
Tallahassee, FL 32306, USA*

and

*Department of Physics, Syracuse University,
Syracuse, NY 13244, USA*

The electroweak diboson production cross-sections are known to receive large radiative corrections beyond leading-order (LO), approaching up to $\sim 60\%$ at next-to-leading order (NLO), compared to the scale uncertainties which are in the range 1-5% at LO. If the scale uncertainties are to be taken seriously, the NLO predictions are as much as $\sim 30\sigma$ away from their LO counterpart suggesting a very poor convergence of the perturbation theory. In this paper, we show that there is a second source of scale uncertainty which has not been considered in the literature, namely the complex phase of the scales, which can lead to large perturbative corrections. Using the formalism of soft-collinear effective theory, we resum these large contributions from the complex phase, finding that the scale uncertainties in fixed-order calculations can be grossly underestimated compared to the resummed predictions, which have uncertainties as large as 13–16% at LO. Even at NLO, we find that the scale uncertainties are marginally higher than previously estimated, depending on the choice of scale. Using our method of scale variation, the compatibility of LO and NLO results within the scale uncertainties is vastly improved so that the perturbation theory can be relied upon. This method of scale variation can be easily extended to beyond NLO calculations as well as other LHC processes.

I. INTRODUCTION

A precise understanding of the electroweak gauge boson pair-production at the LHC is critical for several reasons. First and foremost, many of the diboson processes are dominant backgrounds to Higgs production and its subsequent decays to Standard Model (SM) particles. A good understanding of the diboson background is therefore crucial in the measurement of the Higgs couplings to the SM particles. Secondly, diboson processes constitute an important test for the electroweak sector. And finally, diboson processes are often backgrounds to many new physics processes, making it challenging to distinguish one from the other.

In this paper, we focus on heavy electroweak vector boson pair-production channels, W^+W^- , ZZ and $W^\pm Z$, owing to their similar kinematics. The cross-sections measured by the ATLAS [1–6] and the CMS [7–11] collaborations in these channels at $\sqrt{s} = 7$ TeV and 8 TeV LHC runs are compatible with the theory predictions within 2σ . Three measurements where the discrepancy exceeds 1σ level are the $W^\pm Z$ measurements by CMS and the W^+W^- measurements by both ATLAS and CMS collaborations. The discrepancy in the WW channel is particularly compelling given that both ATLAS and CMS experiments observe an excess of $\sim 20\%$ over the SM theory prediction, which has fueled speculations that new physics could be hiding in the W^+W^- measurements [12–19]. In order to test the possibility of new physics mimicking the SM background, a precise theoretical understanding of the higher-order corrections to the SM diboson production is essential.

The study of higher-order corrections to diboson production has a long history, with the first NLO QCD cor-

rections to W^+W^- , ZZ and $W^\pm Z$ channels computed in [20, 21], [22, 23] and [24], respectively. Leptonic decays of dibosons without spin-correlations was studied in [25]. One-loop helicity amplitudes for leptonic decays of vector boson pair were computed in [26], allowing for complete NLO computation in [27, 28]. The W^+W^- and ZZ cross-sections also receive contributions from the gluon-fusion channel, which although formally NNLO, can be significant owing to large gluon parton distribution functions (PDFs) at the LHC. These corrections were calculated in [29, 30] with the corresponding leptonic decays included in [31–35]. The complete NLO calculations including leptonic decays, spin-correlations and gluon-fusion contributions, for all diboson channels, was presented in [36]. Recently, electroweak calculations have also been considered for W pair-production [37, 38], and for ZZ and $W^\pm Z$ production [39, 40]. NLO QCD corrections to W^+W^- and ZZ production with one jet have been computed in [41–43] and [44], respectively, while $W^+W^- + 2$ jets calculations were considered in [45, 46]. Transverse momentum resummation effects in diboson production have been studied in [47–49], while a jet-veto study for W^+W^- channel was presented in [50]. The threshold corrections arising from soft-gluon resummation were calculated in [51, 52]. Finally, the NNLO QCD corrections to W^+W^- and ZZ have been recently computed in [53] and [54] while the two-loop helicity amplitudes for all diboson channels have been calculated in [55].

Every higher order QCD calculation discussed above includes powers of logarithms of the form $\log [(-M^2 - i0^+)/\mu^2]$ where M is the invariant mass of the diboson system and μ is the factorization scale, which is also the scale at which the PDFs are evaluated. Given that μ dependence of the cross-sections is primarily con-

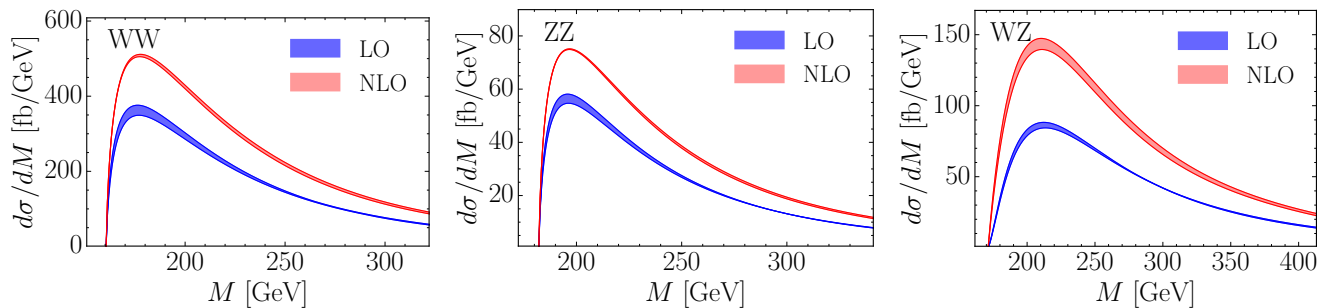


FIG. 1: Differential cross-sections at LO (blue band) and NLO (red band) are shown for W^+W^- (left), ZZ (center) and $W^\pm Z$ (right) production at $\sqrt{s} = 8$ TeV LHC run as obtained from MCFM. The uncertainty bands follow from varying the renormalization and factorization scales as $M/2 < \mu_r = \mu_f < 2M$. Contributions from gluon-fusion channels are not included.

trolled by the logarithmic terms, $\mu \sim M$ seems to be a reasonable choice to minimize the higher order corrections. Further, given that physical observables are μ -independent, one can estimate scale uncertainty in the cross-sections by varying μ . The scale uncertainties in diboson invariant mass distributions at LO and NLO shown in Fig. 1 are obtained by varying the renormalization scale, set equal to the factorization scale ($\mu = \mu_r = \mu_f$), as $M/2 < \mu < 2M$.¹ Contrary to the naive expectations, the NLO perturbative corrections with K-factors in the range 1.4–1.7 [36] far exceed the scale uncertainties. If this scale uncertainty estimate is to be taken seriously, the NLO predictions are as much as $\sim 30\sigma$ away from their corresponding LO values, suggesting that the perturbation theory is very poorly converging.

We argue that there is a second source of scale uncertainty which has not been considered in the literature. If the scale μ is allowed to be complex-valued, there is an additional parameter that must be considered for estimating the scale uncertainties, namely the complex phase of μ^2 . In fact, the logarithms in the higher-order corrections have a branch-cut along the negative real axis, so that $\mu^2 < 0$ is preferred over $\mu^2 > 0$ to minimize logarithms. This is slightly problematic though since the PDFs are necessarily evaluated at $\mu^2 > 0$ leading to large π^2 terms when the logarithms are squared. Summation of π^2 terms has been known for a long time [56–59], and has been recently applied to the case of Higgs production at the LHC [60]. π^2 resummation calculations for diboson production have been performed in the context of threshold resummation for $W^\pm Z$ and ZZ channels [52], and jet-veto resummation for W^+W^- channel [50].

The aim of this paper is to show that the variation in the phase angles of the complex renormalization scales is essential in order to estimate the true scale uncertainties. Just as the variation in the factorization scales is governed by the evolution of the PDFs, the variation of

the phase angle will be governed by a different renormalization group (RG) equation, which we obtain using the formalism of soft-collinear effective theory (SCET) [61–66] by generalizing the concept of π^2 -resummation, where the phase angle is fixed to $(-\pi + 0^+)$, to arbitrary phase angles. While we explicitly focus on heavy vector-boson pair production, our scale variation technique can be extended to any other process once its RG equation is known.²

This paper is organized as follows. In Section II, using the SCET construction for diboson production, we demonstrate that complex-valued scales, not only arise naturally in radiative corrections, but are also associated with large perturbative corrections. In Section III, the large perturbative corrections arising from the complex phases of the scales are resummed to all orders in perturbation theory for W^+W^- , ZZ and $W^\pm Z$ processes, including gluon-fusion production channels, allowing us to study scale variation for complex scales. Finally, in Section IV, our scale variation technique is applied to diboson processes, and numerical results for the diboson production cross-sections are presented for $\sqrt{s} = 7, 8, 13$ and 14 TeV LHC runs.

II. COMPLEX SCALES AND LARGE PERTURBATIVE CORRECTIONS

Any cross-section measurement at the LHC is characterized by a process-dependent *hard*-scale and one or more measurement-kinematics dictated *soft*-scale(s). For example, the *hard*-scale for diboson production is the invariant mass of the boson-pair, M and the *soft*-scale is Λ_{QCD} for an inclusive measurement while jet- p_T measurements introduce another intermediate *soft*-scale, p_T^{jet} . It is well known that the presence of multiple scales in

¹ Varying the scale by factors of 1/2 and 2 around a central value is the standard convention followed in the literature.

² Our analysis is trivially extended to a class of processes which involve colorless final states such as Drell-Yan, as these processes satisfy the same RG equations.

the theory can lead to large logarithms of the ratio of the scales, which can render the perturbation theory invalid. Effective field theories, on the other hand, are adept at dealing with the problem of multiple scales by renormalization group (RG) evolution to a single scale, effectively providing a powerful technique to resum the large logarithms.

As already mentioned before, one such logarithm that appears in the radiative corrections to diboson processes is of the form $\alpha_s^n \log^{2n}[(-M^2 - i0^+)/\mu^2]$, as we will explicitly show later in this section. The structure of the logarithm already motivates us to choose a complex-valued μ^2 . However, the factorization scales at which the PDFs are evaluated are always real valued, so that logarithms take the form $\alpha_s^n [\log(M^2/\mu^2) - i\pi]^{2n}$. Even for the choice of $\mu \approx M$, large perturbative corrections in the form of $\alpha_s^n \pi^{2n}$ terms remain. The question whether such π^2 terms should be resummed or treated as part of non-logarithmic corrections is a highly debated subject, which we will address later in Section III. Nonetheless, it is clear that there exists a hierarchy of scales in the complex μ^2 -plane that lead to large perturbative corrections and should be resummed. We will employ SCET to resum such terms in Section III but first, we set up the basic notation for diboson production in SCET formalism.

Consider the inclusive vector-boson pair production, $pp \rightarrow VV' + X$ where $V, V' \in \{W, Z\}$ and X is any hadronic final state. We will primarily focus on the process $q\bar{q}' \rightarrow VV'$ which is the only production channel at LO. Throughout this paper, we extensively follow the SCET construction and notation used in [50], which we refer to the interested readers for more details. Let us begin by writing down the SCET Lagrangian for VV' production :

$$\mathcal{L} = \frac{1}{M} [\epsilon_\mu^V]^* [\epsilon_\nu^{V'}]^* e^{i(p_V + p_{V'}) \cdot x} \mathcal{J}^{\mu\nu}(x) \quad (1)$$

where ϵ_μ are the spin and momentum dependent gauge-boson polarization vectors, p_V and $p_{V'}$ are the gauge-boson four momenta, and \mathcal{J} , the SCET operator describing the interaction of incoming ‘quark-jets’ with the external outgoing gauge bosons, is given by

$$\mathcal{J}^{\mu\nu}(x) = \int dt_1 dt_2 \left[C^{\mu\nu}(t_1, t_2, p_V, p_{V'}, \mu) \times \chi_{\bar{c}}^\alpha(x^- + t_2) \Gamma_\alpha^\beta \chi_{c\beta}(x^+ + t_1) \right] \quad (2)$$

Here, $\chi_c(\chi_{\bar{c}})$ is a gauge-invariant collinear (anti-collinear) quark field in SCET ³, Γ is a spinor structure explicitly defined in [50] and $C^{\mu\nu}$ is the Wilson coefficient of the SCET operator which is a function of gauge boson momenta, the RG scale μ as well as the spatial parameters

t_1 and t_2 along the light-cone directions as allowed by the non-locality of the SCET operators. In the above expression, the spinor indices have been made explicit, while the color and flavor indices are implicit. The multipole expansion of the operators in Eq. (2), as dictated by requiring inclusive measurements, is slightly different from that in [50] where jet-veto condition is imposed. Nonetheless, the hard coefficients which appear in the factorized SCET cross-sections for $q\bar{q}' \rightarrow VV'$ production are the same in either case, and ultimately the only ingredients affected by the resummation in the complex μ^2 -plane, as we will show later. They are given by

$$C(\mu) = \tilde{C}^{\mu\nu} [\tilde{C}^{\rho\sigma}]^* [\epsilon_\mu^V]^* [\epsilon_\nu^{V'}]^* \epsilon_\rho^V \epsilon_\sigma^{V'} \quad (3)$$

where, $\tilde{C}^{\mu\nu}$ is the Fourier-transform of the position space Wilson coefficients $C^{\mu\nu}$ which appear in Eq. (2). For brevity, here and throughout the rest of the paper, the quark flavor, helicity and momentum dependence of the hard coefficients will be suppressed. Also implicit are the gauge-boson spin and momentum dependence on the RHS of the above equation, including the summation over the final state spins.

A typical SCET calculation for LHC observables involves computing the Wilson coefficients by matching the SCET operators to the full QCD at a *hard* scale μ_h , and then RG evolving the coefficients to a factorization scale μ_f at which the PDFs are evaluated, where the second step resums the large logarithms of the ratio μ_h/μ_f . For VV' production, the hard coefficient at one-loop takes the following form at the matching scale μ_h [50]:

$$C(\mu_h) = \left[1 - \frac{C_F \alpha_s(\mu_h)}{4\pi} \left(2L_M^2(\mu_h) - 6L_M(\mu_h) + \frac{\pi^2}{3} \right) \right] |\mathcal{M}_0|^2 + \frac{C_F \alpha_s(\mu_h)}{2\pi} \text{Re}(\mathcal{M}_0^* \mathcal{M}_{1,\text{reg}}) \quad (4)$$

where, $L_M(\mu) = \log[(-M^2 - i0^+)/\mu^2]$, \mathcal{M}_0 is the Born-level amplitude for the process $q\bar{q}' \rightarrow VV'$, and $\mathcal{M}_{1,\text{reg}}$ is the one-loop amplitude for the same process with the IR poles subtracted using the $\overline{\text{MS}}$ scheme. As already discussed before, an optimal choice for the matching scale μ_h that minimizes the higher order corrections arising from the logarithms $L_M(\mu_h)$ is $\mu_h^2 \sim M^2 e^{-i(\pi-0^+)}$, rather than $\mu_h^2 \sim M^2$ [56–60]. On the other hand, the PDFs (or more generally ‘beam-functions’ [67, 68] for less inclusive observables) that multiply the hard coefficients in the cross-sections are typically evaluated at factorization scales, μ_f which are real valued, in contrast to our optimal choice of the matching scale which is phase-shifted by π in the complex μ^2 -plane. Therefore, even for the case $\mu_f = |\mu_h|$, there exists a hierarchy of scales in the complex μ^2 -plane leading to large perturbative corrections that need to be resummed, which we discuss in the next section.

³ The gauge invariance of χ_c and $\chi_{\bar{c}}$ is implemented by dressing the bare quark fields with collinear gluon Wilson lines [61–63].

III. RESUMMATION AND SCALE VARIATION

Before we describe the resummation of large perturbative terms associated with the complex phase of μ^2 , let us define the hierarchy of scales more precisely. For a typical measurement involving VV' final states, inclusive or otherwise, there are at least two scales in the problem: the hard scale, μ_h and the factorization scale, μ_f .⁴ Given that μ_h is complex-valued, the RG evolution of the hard coefficients can be realized as a two step process, $C(\mu_h) \rightarrow C(|\mu_h|) \rightarrow C(\mu_f)$. In this paper, we will consider inclusive cross-sections so that it is reasonable to set $\mu_f = |\mu_h| \equiv \mu$. For less inclusive measurements, such as imposing jet-veto [50], we have $\mu_f \neq |\mu_h|$ so that the evolution $C(|\mu_h|) \rightarrow C(\mu_f)$ must also be considered. Nevertheless, the first RG running, $C(\mu_h) \rightarrow C(|\mu_h|)$ essentially decouples from the second RG running, $C(|\mu_h|) \rightarrow C(\mu_f)$, so that our analysis can be trivially extended to less-inclusive measurements.

Let us define $\mu \equiv \mu_f = |\mu_h|$ and $\mu_h^2 = \mu^2 e^{i\Theta}$, where $\Theta \in (-\pi, \pi)$ is the complex phase angle. In the last section, we showed that the logarithms $L_M(\mu_h)$ present in the hard matching coefficient are minimized for $\mu = M$ and $\Theta = -\pi + 0^+$. While the effective field theory dictates the choice of the hard matching scale to be the scale of the hard interaction such that $\mu = \mathcal{O}(M)$ and $\Theta = \mathcal{O}(-\pi)$, there is nonetheless an ambiguity associated with the choice of the hard scale parameters, μ and Θ , since the contribution of non-logarithmic terms in Eq. (4) maybe sizable. On the other hand, total cross-section, being a physical observable, is independent of the choice of matching scale. Therefore, this ambiguity in the choice of matching scale parameters should be reflected as scale uncertainty in the theory prediction.

Variation of the hard scale in the complex μ^2 -plane is shown in Fig. 2, where the shaded annulus corresponds to the region $M/2 < \mu < 2M$ and $-\pi < \Theta < \pi$. If the non-logarithmic terms in Eq. (4) were completely dominant over the logarithmic ones, there would be no preferred value of Θ . On the other extreme, if logarithmic terms were completely dominant, $\Theta = -\pi + 0^+$ would be the ideal choice. Numerically, for the diboson processes, we find that π^2 terms arising from the logarithms account for nearly a half of the total NLO corrections, so that the situation is somewhere in between. With these considerations in mind, to estimate the scale uncertainties for diboson processes, we select the region $-\pi < \Theta < 0$ as indicated by the green hatched region in Fig. 2. This is to be contrasted with the fixed-order calculations which have $\Theta = 0$ on one hand, and π^2 -resummation calcula-

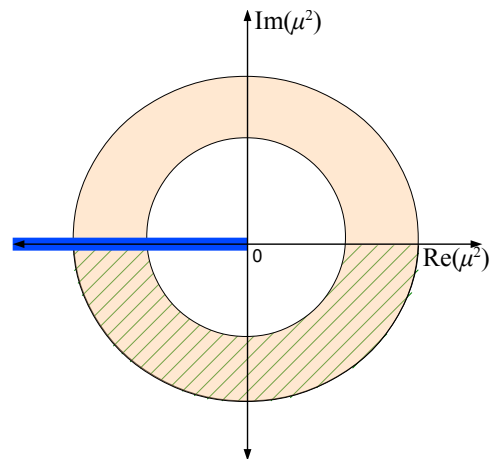


FIG. 2: Variation of the hard scale μ_h is shown in the complex μ^2 -plane with a branch cut along the negative real axis. The orange shaded region satisfies $M/2 < |\mu_h| < 2M$ but only the hatched region of the annulus is considered for scale variation.

tions which select $\Theta = -\pi + 0^+$ on the other hand.

For the process $q\bar{q}' \rightarrow VV'$, the scale dependence of the hard coefficients in Eq. (3) follows from that of the Wilson coefficients, which in turn satisfy the following RG equation :

$$\mu \frac{d\tilde{C}^{\mu\nu}(\mu)}{d\mu} = \left(\Gamma_F^{\text{cusp}} L_M(\mu) + 2\gamma_F \right) \tilde{C}^{\mu\nu}(\mu) \quad (5)$$

where Γ_F^{cusp} is the cusp-anomalous dimension which resums double logarithms while γ_F is the anomalous dimension which resums single logarithms. Both Γ_F^{cusp} and γ_F implicitly depend on μ through α_s . The anomalous dimensions appearing in the RG equation above are universal for class of processes which have colorless final states (not counting emissions from initial state quarks), and therefore identical for all diboson production processes and Drell-Yan.

A subtlety that emerges from the RG running between the scales μ_h and μ_f is that the strong coupling $\alpha_s(\mu)$ must now be defined in the complex μ^2 -plane with a branch cut along the negative real axis. As long as the contours of integration are sufficiently away from the Landau pole in the complex μ^2 -plane, $\alpha_s(\mu)$ is well-defined along such contours. Using the definition of QCD beta function $\beta(\alpha_s)$ and performing contour integration, a particularly useful result can be obtained [60] :

$$\int_{\alpha_s(\mu)}^{\alpha_s(\mu_h)} \frac{d\alpha_s}{\beta(\alpha_s)} = \frac{i\Theta}{2} \quad (6)$$

For the purpose of power counting in α_s , we shall treat $|\Theta| \sim \mathcal{O}(\alpha_s^{-1})$ although numerically Θ can also be zero. Eq. (6) allows us to compute the complex couplings $\alpha_s(\mu_h)$ in terms of the real couplings $\alpha_s(\mu)$, where the latter can be computed in a standard way. At NLO, we

⁴ More generally, one can consider a soft scale $\mu_s \sim \Lambda_{QCD}$ but we assume that the evolution from $\mu = \mu_s$ to $\mu = \mu_f$ is accounted by the PDF running. This is true when the ‘threshold corrections’ from soft-emissions are small, which has been shown for the diboson processes [51, 52].

have the following relation :

$$\frac{\alpha_s(\mu)}{\alpha_s(\mu_h)} = 1 + ia(\mu)\frac{\Theta}{\pi} + \frac{\alpha_s(\mu)}{4\pi}\frac{\beta_1}{\beta_0}\log\left[1 + ia(\mu)\frac{\Theta}{\pi}\right] + \mathcal{O}(\alpha_s^2) \quad (7)$$

where $a(\mu) = \beta_0\alpha_s(\mu)/4$ and $\beta_0 = 11/3C_A - 4/3T_F n_f$ with $C_A = 4$, $T_F = 1/2$ and n_f is the active number of flavors which we take to be five. Numerically, since $a(\mu) \approx 0.2$, Eq. (7) is a good approximation even at NNLO.

Having addressed the subtleties associated with complex values of μ^2 , we can solve the RG equation in Eq. (5) to evolve the Wilson coefficients from $\mu = \mu_h$ to $\mu = \mu$

$$\tilde{C}^{\mu\nu}(\mu) = \mathcal{U}(\mu, \mu_h)\tilde{C}^{\mu\nu}(\mu_h) \quad (8)$$

where, the analytical expression for the evolution kernel \mathcal{U} can be found in [50, 69]. Counting Θ as $\mathcal{O}(\alpha_s^{-1})$ and neglecting $\mathcal{O}(\alpha_s)$ and higher-order terms in $\log\mathcal{U}$, to a good approximation we have [60],

$$\log|\mathcal{U}(\mu, \mu_h)|^2 \approx \frac{\Gamma_0^F\Theta^2\alpha_s(\mu)}{8\pi}\left[1 + \frac{\alpha_s(\mu)}{4\pi}\left\{\frac{\Gamma_1^F}{\Gamma_0^F} - \frac{2\beta_0\gamma_0^F}{\Gamma_0^F} - \beta_0\log\left(\frac{M^2}{\mu^2}\right)\right\}\right] \quad (9)$$

In the above equation, $\Gamma_0^F = 4C_F$, $\gamma_0^F = -3C_F$,

$$\Gamma_1^F = 4C_F\left[C_A\left(\frac{67}{9} - \frac{\pi^2}{3}\right) - \frac{20}{9}T_F n_f\right] \quad (10)$$

where, $C_F = 4/3$ and the remaining symbols have already been defined below Eq. (7). It has been shown in [60] that the impact of including $\mathcal{O}(\alpha_s)$ and higher-order terms in $\log|\mathcal{U}|^2$ is small so that Eq. (9) is a good approximation even at higher-orders. Before concluding this section, we briefly comment on the diboson production from the gluon-fusion channel.

Gluon-induced Diboson Production

W^+W^- and ZZ production cross-sections get contributions from gg channel, which although formally NNLO, can be sizable at the LHC owing to large gluon PDFs. Although higher-order corrections to the process $gg \rightarrow VV'$ are currently unknown, they are expected to be large, as has been established for the case of Higgs production in the gluon-fusion channel where the NNLO K-factors can be as big as ~ 2.5 . In [60], it was shown that the bulk of such large K-factors stem from the π^2 enhanced terms. It is then reasonable to expect that the scale uncertainties in the theory predictions for $gg \rightarrow VV'$ process would be grossly underestimated if the scale variation in the complex μ^2 -plane is not considered. The origin of large perturbative correction from complex-valued scales in gluon-induced diboson production as well

as their resummation is identical to the arguments presented above for the $q\bar{q}'$ channel, which we briefly outline below.

The SCET Lagrangian for the $gg \rightarrow VV'$ process is similar to Eq. (1) with the SCET operator \mathcal{J} now describing the interaction of incoming ‘gluon-jets’ with the outgoing electroweak gauge bosons. Analogous to Eq. (2), \mathcal{J} is constructed using gauge-invariant collinear and anti-collinear SCET gluon fields, \mathcal{A}_c^μ and $\mathcal{A}_{\bar{c}}^\mu$. The hard coefficients analogous to Eq. (3) are only known at LO for the $gg \rightarrow VV'$ processes, however, their RG evolution is identical to that of the hard coefficient for the Higgs production, $gg \rightarrow h$. Therefore, it is possible to resum the large perturbative terms associated with the complex phase of μ^2 , so that a realistic estimate of the scale uncertainty can be obtained. The evolution kernel $\mathcal{U}(\mu, \mu_h)$ required for the computation can be found in [60], which to a good approximation is given by

$$\log|\mathcal{U}(\mu, \mu_h)|^2 \approx \frac{\Gamma_0^A\Theta^2\alpha_s(\mu)}{8\pi}\left[1 + \frac{\alpha_s(\mu)}{4\pi}\left\{\frac{\Gamma_1^A}{\Gamma_0^A} - \beta_0\log\left(\frac{M^2}{\mu^2}\right)\right\}\right] \quad (11)$$

where, $\Gamma_0^A = 4C_A$ and Γ_1^A is given by the same expression as Γ_1^F in Eq. (10) but with C_F replaced by C_A .

To summarize this section, we have calculated the evolution kernels $\mathcal{U}(\mu, \mu_h)$, which resum the large perturbative corrections arising from the complex phase of the hard scale μ_h . In the next section, we will show how to combine these kernels with the existing LO and NLO codes such as MCFM, to estimate the true scale uncertainties and the central values for theory prediction of the diboson cross-sections.

IV. RESULTS

In order to incorporate our scale variation technique into existing fixed-order calculations, we require differential cross-sections in M . Presently, only NLO $q\bar{q}' \rightarrow VV'$ and LO $gg \rightarrow VV'$ differential distributions are publicly available. All our numerical results will extensively use the MCFM program for extracting the fixed-order differential cross-sections with MSTW2008 [70] as the choice for PDF sets. Implementing scale variation in the full complex μ^2 -plane requires computation of cross-section where the large perturbative corrections from the complex phase, Θ have been resummed. At LO, this is implemented as follows:

$$\frac{d\sigma^{\text{LO}}}{dM}(\Theta, \mu, M) = |\mathcal{U}(\Theta, \mu, M)|^2 \frac{d\sigma^{\text{LO}}}{dM}(\mu, M) \quad (12)$$

where, $\mathcal{U}(\Theta, \mu, M) \equiv \mathcal{U}(\mu, \mu_h)$ is the evolution kernel defined in Eq. (9) for the $q\bar{q}'$ channel and Eq. (11) for the gg channel. The computation of kernels requires $\alpha_s(\mu)$ which we obtain from NNLO PDF sets. The differential cross-section on the RHS of the above equation is

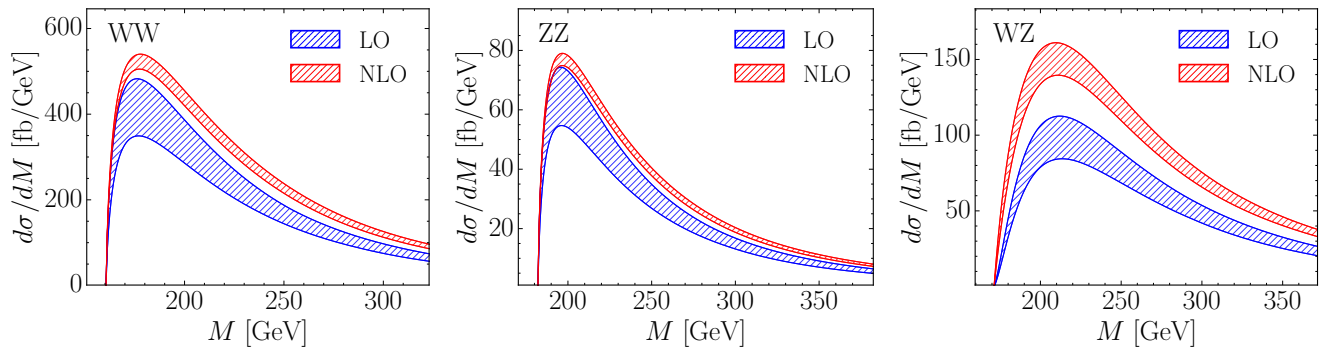


FIG. 3: Differential cross-sections at LO (blue hatched bands) and NLO (red hatched band) are shown for W^+W^- (left), ZZ (center) and $W^\pm Z$ (right) production at $\sqrt{s} = 8$ TeV LHC obtained from our scale variation method in the complex μ^2 -plane as described in the text. Contributions from gluon-fusion channels are not included.

obtained from MCFM using LO PDF sets with the factorization scale $\mu_f = \mu$. By varying the parameters $M/2 < \mu < 2M$ and $-\pi < \Theta < 0$, we therefore obtain the scale variation in the complex μ^2 -plane.

Implementation of our method at NLO follows similarly, however, appropriate subtractions must be made to avoid double-counting since $\mathcal{O}(\alpha_s)$ contributions associated with the phase Θ are already a part of NLO. To do so, we remove $\mathcal{O}(\alpha_s)$ expansion of the kernels \mathcal{U} from the fixed-order NLO results, before implementing resummation. We therefore arrive at the following formula for the process $q\bar{q}' \rightarrow VV'$ at NLO:

$$\frac{d\sigma^{\text{NLO}}}{dM}(\Theta, \mu, M) = |\mathcal{U}(\Theta, \mu, M)|^2 \left[\frac{d\sigma^{\text{NLO}}}{dM}(\mu, M) - \frac{\Gamma_0^{\text{F}} \Theta^2 \alpha_s(\mu)}{8\pi} \frac{d\sigma^{\text{LO}}}{dM}(\mu, M) \right] \quad (13)$$

where, all quantities in the square bracket are computed using NLO PDF sets. The differential cross-sections on the RHS of the above equation are again obtained from MCFM by setting the renormalization and factorization scales as $\mu_r = \mu_f = \mu$. We are now in a position to present the numerical results for diboson production using our scale variation method.

	7 TeV	8 TeV	13 TeV	14 TeV
σ_{WW}^{LO} [pb]	33.8 ± 4.3	41.2 ± 5.5	82.5 ± 13.2	91.4 ± 15.0
σ_{WW}^{NLO} [pb]	45.3 ± 2.2	55.2 ± 2.6	109.1 ± 4.5	120.7 ± 5.0
σ_{WW}^{gg} [pb]	1.6 ± 0.7	2.1 ± 1.0	6.0 ± 2.7	7.0 ± 3.1

TABLE I: LO and NLO cross-section predictions for W^+W^- production at $\sqrt{s} = 7, 8, 13$ and 14 TeV LHC runs, using our scale-variation method. The contribution of gluon-fusion channel is shown separately.

The total LO and NLO cross-sections, along with their scale uncertainties, for W^+W^- , ZZ and $W^\pm Z$ produc-

	7 TeV	8 TeV	13 TeV	14 TeV
σ_{ZZ}^{LO} [pb]	4.7 ± 0.6	5.8 ± 0.7	11.9 ± 1.8	13.2 ± 2.1
σ_{ZZ}^{NLO} [pb]	6.0 ± 0.2	7.3 ± 0.2	14.6 ± 0.4	16.2 ± 0.4
σ_{ZZ}^{gg} [pb]	0.5 ± 0.2	0.7 ± 0.3	1.9 ± 0.9	2.2 ± 1.0

TABLE II: Same as Table I but for ZZ production.

	7 TeV	8 TeV	13 TeV	14 TeV
$\sigma_{W^\pm Z}^{\text{LO}}$ [pb]	7.8 ± 1.0	9.4 ± 1.1	18.4 ± 2.6	20.3 ± 3.0
$\sigma_{W^\pm Z}^{\text{NLO}}$ [pb]	11.6 ± 0.8	14.2 ± 1.0	28.3 ± 1.9	31.6 ± 2.3
$\sigma_{W^\pm Z}^{\text{LO}}$ [pb]	4.2 ± 0.5	5.3 ± 0.6	11.3 ± 1.6	12.7 ± 1.9
$\sigma_{W^\pm Z}^{\text{NLO}}$ [pb]	6.5 ± 0.5	8.2 ± 0.6	18.3 ± 1.4	20.3 ± 1.4

TABLE III: Same as Table I but for $W^\pm Z$ production. There is no gluon-fusion production channel for this process.

tion at different center of mass energy LHC runs are presented in Table I, Table II and Table III, respectively. The gluon-fusion contribution for W^+W^- and ZZ processes is also shown in these tables. Besides the scale uncertainties shown in the tables, there are additional theoretical uncertainties of $\sim 3\text{--}4\%$ from the PDFs. In Fig. 3, LO and NLO differential cross-sections are shown for W^+W^- , ZZ and $W^\pm Z$ production in the $q\bar{q}'$ channel at $\sqrt{s} = 8$ TeV LHC run using the complex scale variation technique described earlier in this section. This is to be contrasted with Fig. 1 where traditional approach ($M/2 < \mu < 2M$) for estimating the scale uncertainties was followed. We conclude with the following remarks:

- First and foremost, we find that the scale uncertainties are grossly underestimated in Fig. 1, corroborating our argument that variation in the full complex μ^2 -plane must be considered in order to estimate the true scale uncertainties. As can be

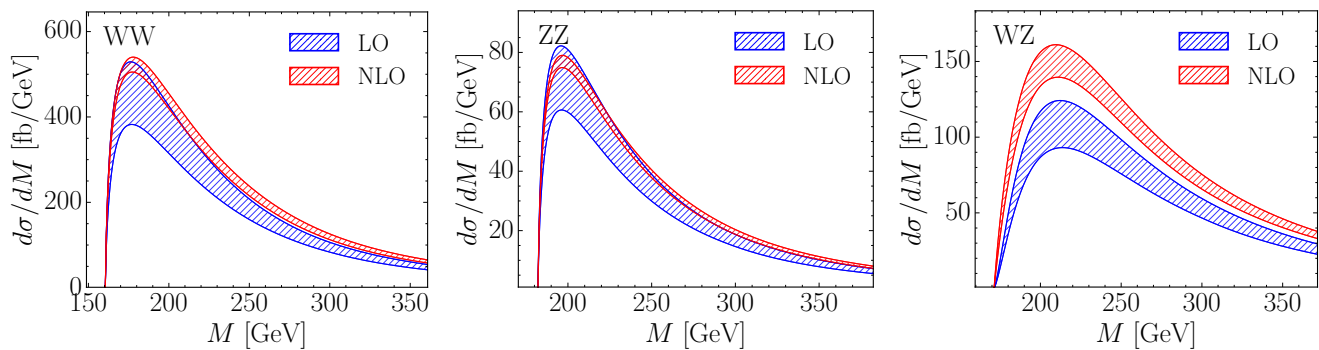


FIG. 4: Same as Fig. 3 but NLO PDF set is used for both LO and NLO cross-sections.

seen in Fig. 3, the effect is striking at LO, with uncertainties in the range 13–16% in contrast to the traditional approach which estimate the uncertainties to be 2–4%. This is particularly relevant for diboson production in gluon-fusion channels which, although formally NNLO, is absent at lower orders, thus suffering from the same scale uncertainty underestimation issues as LO $q\bar{q}'$ channel. Even at NLO, the scale uncertainties using our method are 3–4% higher compared to previous fixed-order estimates with $M/2 < \mu < 2M$. Most importantly, NLO predictions for all diboson processes are now less than 5σ away from their LO value, giving us confidence in the reliability of the perturbation theory.

- Owing to the large scale uncertainties in our method of scale variation, the central value predictions for LO and NLO cross-sections are also altered. We assign the central value to be the center of the uncertainty band so that all the numerical results presented in this section have symmetrical error bars. Our best prediction for LO cross-sections are 15% (46%) higher than the previous fixed-order predictions for $q\bar{q}'$ (gg) channel. At NLO, we find a marginal increase of 3–4% for the $q\bar{q}'$ channel.
- Up to this point, we have compared our results with fixed-order calculations that use dynamic scales, $M/2 < \mu < 2M$. We now compare our results with fixed-order predictions that use a rather ad-hoc choice for the renormalization and factorization scales $\bar{m}/2 < \mu < 2\bar{m}$, where \bar{m} is the average mass of the vector bosons V and V' [36]. At LO, the fixed-order calculations fail miserably as expected, predicting scale uncertainty as low as 1%. However, at NLO, the fixed-order calculations work surprisingly well with their central-value predictions within 2% of our results for all diboson processes. The scale uncertainties in these calculations are marginally underestimated by 2–4% with the largest discrepancy with our method arising for the $W^\pm Z$ process. In general, we expect that our

method assigns larger scale uncertainty to processes with large K-factor.

- While we have consistently used LO PDF set for LO cross-sections and NLO PDF set for NLO cross-sections, it is worthwhile to gauge the impact of the order of PDF on higher-order corrections. In Fig. 4, we present our results using NLO PDF set for both LO and NLO computations. Clearly, a significant portion of higher order corrections to diboson processes is driven by the radiative corrections to the PDF.
- As we already discussed, closely related calculations have appeared in the literature before under the name of π^2 -resummation, where the complex phase is held fixed at $\Theta = -\pi + 0^+$. π^2 -resummation for ZZ and $W^\pm Z$ channels was performed in [52] leading to an increase over fixed-order NLO predictions by 4% and 8% respectively. Given that we vary $-\pi < \Theta < 0$, such an enhancement appears as an upper limit of our scale variation, with an increase in our central value prediction being nearly half of that from π^2 -resummation. Similar calculations for W^+W^- production in the 0-jet bin [50] reveal impact of π^2 -resummation to be $\sim 7\%$ beyond NLO, thus partly explaining the slight excess in the W^+W^- cross-section measurement compared to the theory prediction⁵.
- Recently, NNLO calculations have been performed for W^+W^- [53] and ZZ [54] processes, although differential distributions in M are not publicly available so that our scale variation technique can not be applied at the moment. It would nevertheless be an interesting check if the choice of scale

⁵ The other factor possibly responsible for the discrepancy between the experiment and the theory predictions of W^+W^- cross-section is the jet-veto efficiency which has been explored in [49, 50, 71].

considered in these calculations, $\overline{m}/2 < \mu < 2\overline{m}$, can mimic our method even at NNLO. It should be noted that the increase beyond NLO from π^2 -resummation discussed above is comparable to that from full NNLO calculations for both W^+W^- and ZZ channels suggesting that π^2 terms dominate even beyond NLO. We have already pointed out that there are production channels, which open up only at higher orders, for which scale uncertainties would be underestimated. One such channel is the gluon-fusion mode at NNLO for which we have explicitly presented the central value and the scale uncertainties.

- Finally, we point out that our scale-variation technique can be easily incorporated when considering other higher order calculations to diboson processes by simply modifying Eq. (13). For fixed order calculations, one simply has to replace $d\sigma/dM$, while for resummation calculations, the evolution kernel \mathcal{U} also gets modified. In particular, there are two scenarios where large perturbative corrections

from complex-phase of the scales is partially cancelled at large M . As shown in [37–40], for large M , electroweak Sudakov logarithms of the form $\alpha \log^2(M_V/M)$ and $\alpha \log(M_V/M)$ can lead to large negative corrections to diboson cross-sections. Another scenario where cancellation at large M is realized is the presence of jet-vetoes, where logarithms of the form $\alpha_s \log^2(p_T^{\text{veto}}/M)$ and $\alpha_s \log(p_T^{\text{veto}}/M)$ again lead to large negative corrections [50]. Further, our method of scale variation can be easily extended to beyond NLO calculations as well as to other LHC processes, involving more complicated colored structures in the final states.

Acknowledgements

The author would like to thank Sally Dawson, Patrick Meade, Takemichi Okui and George Sterman for useful discussions and comments on the manuscript.

-
- [1] *Measurement of the W^+W^- production cross section in proton-proton collisions at $\sqrt{s} = 8$ TeV with the ATLAS detector*, Tech. Rep. ATLAS-CONF-2014-033 (CERN, Geneva, 2014).
- [2] *Measurement of the total ZZ production cross section in proton-proton collisions at $\sqrt{s} = 8$ TeV in 20 fb^{-1} with the ATLAS detector*, Tech. Rep. ATLAS-CONF-2013-020 (CERN, Geneva, 2013).
- [3] *A Measurement of WZ Production in Proton-Proton Collisions at $\sqrt{s}=8\text{TeV}$ with the ATLAS Detector*, Tech. Rep. ATLAS-CONF-2013-021 (CERN, Geneva, 2013).
- [4] G. Aad *et al.* (ATLAS), *Phys.Rev.* **D87**, 112001 (2013), arXiv:1210.2979 [hep-ex] .
- [5] G. Aad *et al.* (ATLAS), *JHEP* **1303**, 128 (2013), arXiv:1211.6096 [hep-ex] .
- [6] G. Aad *et al.* (ATLAS), *Eur.Phys.J.* **C72**, 2173 (2012), arXiv:1208.1390 [hep-ex] .
- [7] S. Chatrchyan *et al.* (CMS Collaboration), *Phys.Lett.* **B721**, 190 (2013), arXiv:1301.4698 [hep-ex] .
- [8] V. Khachatryan *et al.* (CMS Collaboration), (2014), arXiv:1406.0113 [hep-ex] .
- [9] *Measurement of WZ production rate*, Tech. Rep. CMS-PAS-SMP-12-006 (CERN, Geneva, 2013).
- [10] S. Chatrchyan *et al.* (CMS Collaboration), *Eur.Phys.J.* **C73**, 2610 (2013), arXiv:1306.1126 [hep-ex] .
- [11] S. Chatrchyan *et al.* (CMS Collaboration), *JHEP* **1301**, 063 (2013), arXiv:1211.4890 [hep-ex] .
- [12] B. Feigl, H. Rzehak, and D. Zeppenfeld, *Phys.Lett.* **B717**, 390 (2012), arXiv:1205.3468 [hep-ph] .
- [13] D. Curtin, P. Jaiswal, and P. Meade, *Phys.Rev.* **D87**, 031701 (2013), arXiv:1206.6888 [hep-ph] .
- [14] P. Jaiswal, K. Kopp, and T. Okui, *Phys.Rev.* **D87**, 115017 (2013), arXiv:1303.1181 [hep-ph] .
- [15] K. Rolbiecki and K. Sakurai, *JHEP* **1309**, 004 (2013), arXiv:1303.5696 [hep-ph] .
- [16] D. Curtin, P. Jaiswal, P. Meade, and P.-J. Tien, *JHEP* **1308**, 068 (2013), arXiv:1304.7011 [hep-ph] .
- [17] D. Curtin, P. Meade, and P.-J. Tien, (2014), arXiv:1406.0848 [hep-ph] .
- [18] J. S. Kim, K. Rolbiecki, K. Sakurai, and J. Tattersall, (2014), arXiv:1406.0858 [hep-ph] .
- [19] H. Luo, M.-x. Luo, K. Wang, T. Xu, and G. Zhu, (2014), arXiv:1407.4912 [hep-ph] .
- [20] J. Ohnemus, *Phys.Rev.* **D44**, 1403 (1991).
- [21] S. Frixione, *Nucl.Phys.* **B410**, 280 (1993).
- [22] J. Ohnemus and J. Owens, *Phys.Rev.* **D43**, 3626 (1991).
- [23] B. Mele, P. Nason, and G. Ridolfi, *Nucl.Phys.* **B357**, 409 (1991).
- [24] S. Frixione, P. Nason, and G. Ridolfi, *Nucl.Phys.* **B383**, 3 (1992).
- [25] J. Ohnemus, *Phys.Rev.* **D50**, 1931 (1994), arXiv:hep-ph/9403331 [hep-ph] .
- [26] L. J. Dixon, Z. Kunszt, and A. Signer, *Nucl.Phys.* **B531**, 3 (1998), arXiv:hep-ph/9803250 [hep-ph] .
- [27] J. M. Campbell and R. K. Ellis, *Phys.Rev.* **D60**, 113006 (1999), arXiv:hep-ph/9905386 [hep-ph] .
- [28] L. J. Dixon, Z. Kunszt, and A. Signer, *Phys.Rev.* **D60**, 114037 (1999), arXiv:hep-ph/9907305 [hep-ph] .
- [29] E. N. Glover and J. van der Bij, *Phys.Lett.* **B219**, 488 (1989).
- [30] D. A. Dicus, C. Kao, and W. Repko, *Phys.Rev.* **D36**, 1570 (1987).
- [31] T. Matsuura and J. van der Bij, *Z.Phys.* **C51**, 259 (1991).
- [32] C. Zecher, T. Matsuura, and J. van der Bij, *Z.Phys.* **C64**, 219 (1994), arXiv:hep-ph/9404295 [hep-ph] .
- [33] T. Binoth, N. Kauer, and P. Mertsch, , 142 (2008), arXiv:0807.0024 [hep-ph] .
- [34] T. Binoth, M. Ciccolini, N. Kauer, and M. Kramer, *JHEP* **0503**, 065 (2005), arXiv:hep-ph/0503094 [hep-ph] .
- [35] T. Binoth, M. Ciccolini, N. Kauer, and M. Kramer, *JHEP* **0612**, 046 (2006), arXiv:hep-ph/0611170 [hep-ph] .

- [36] J. M. Campbell, R. K. Ellis, and C. Williams, *JHEP* **1107**, 018 (2011), arXiv:1105.0020 [hep-ph] .
- [37] A. Bierweiler, T. Kasprzik, J. H. Khn, and S. Uccirati, *JHEP* **1211**, 093 (2012), arXiv:1208.3147 [hep-ph] .
- [38] M. Billoni, S. Dittmaier, B. Jger, and C. Speckner, *JHEP* **1312**, 043 (2013), arXiv:1310.1564 [hep-ph] .
- [39] A. Bierweiler, T. Kasprzik, and J. H. Khn, *JHEP* **1312**, 071 (2013), arXiv:1305.5402 [hep-ph] .
- [40] J. Baglio, L. D. Ninh, and M. M. Weber, *Phys.Rev.* **D88**, 113005 (2013), arXiv:1307.4331 .
- [41] S. Dittmaier, S. Kallweit, and P. Uwer, *Phys.Rev.Lett.* **100**, 062003 (2008), arXiv:0710.1577 [hep-ph] .
- [42] J. M. Campbell, R. K. Ellis, and G. Zanderighi, *JHEP* **0712**, 056 (2007), arXiv:0710.1832 [hep-ph] .
- [43] S. Dittmaier, S. Kallweit, and P. Uwer, *Nucl.Phys.* **B826**, 18 (2010), arXiv:0908.4124 [hep-ph] .
- [44] T. Binoth, T. Gleisberg, S. Karg, N. Kauer, and G. Sanguinetti, *Phys.Lett.* **B683**, 154 (2010), arXiv:0911.3181 [hep-ph] .
- [45] T. Melia, K. Melnikov, R. Rontsch, and G. Zanderighi, *Phys.Rev.* **D83**, 114043 (2011), arXiv:1104.2327 [hep-ph] .
- [46] N. Greiner, G. Heinrich, P. Mastrolia, G. Ossola, T. Reiter, *et al.*, *Phys.Lett.* **B713**, 277 (2012), arXiv:1202.6004 [hep-ph] .
- [47] Y. Wang, C. S. Li, Z. L. Liu, D. Y. Shao, and H. T. Li, *Phys.Rev.* **D88**, 114017 (2013), arXiv:1307.7520 .
- [48] M. Grazzini, *JHEP* **0601**, 095 (2006), arXiv:hep-ph/0510337 [hep-ph] .
- [49] P. Meade, H. Ramani, and M. Zeng, (2014), arXiv:1407.4481 [hep-ph] .
- [50] P. Jaiswal and T. Okui, (2014), arXiv:1407.4537 [hep-ph] .
- [51] S. Dawson, I. M. Lewis, and M. Zeng, *Phys.Rev.* **D88**, 054028 (2013), arXiv:1307.3249 .
- [52] Y. Wang, C. S. Li, Z. L. Liu, and D. Y. Shao, *Phys.Rev.* **D90**, 034008 (2014), arXiv:1406.1417 [hep-ph] .
- [53] T. Gehrmann, M. Grazzini, S. Kallweit, P. Maierhfer, A. von Manteuffel, *et al.*, (2014), arXiv:1408.5243 [hep-ph] .
- [54] F. Cascioli, T. Gehrmann, M. Grazzini, S. Kallweit, P. Maierhfer, *et al.*, *Phys.Lett.* **B735**, 311 (2014), arXiv:1405.2219 [hep-ph] .
- [55] F. Caola, J. M. Henn, K. Melnikov, A. V. Smirnov, and V. A. Smirnov, (2014), arXiv:1408.6409 [hep-ph] .
- [56] G. Parisi, *Phys.Lett.* **B90**, 295 (1980).
- [57] G. F. Sterman, *Nucl.Phys.* **B281**, 310 (1987).
- [58] L. Magnea and G. F. Sterman, *Phys.Rev.* **D42**, 4222 (1990).
- [59] T. O. Eynck, E. Laenen, and L. Magnea, *JHEP* **0306**, 057 (2003), arXiv:hep-ph/0305179 [hep-ph] .
- [60] V. Ahrens, T. Becher, M. Neubert, and L. L. Yang, *Phys.Rev.* **D79**, 033013 (2009), arXiv:0808.3008 [hep-ph] .
- [61] C. W. Bauer, S. Fleming, and M. E. Luke, *Phys.Rev.* **D63**, 014006 (2000), arXiv:hep-ph/0005275 [hep-ph] .
- [62] C. W. Bauer, S. Fleming, D. Pirjol, and I. W. Stewart, *Phys.Rev.* **D63**, 114020 (2001), arXiv:hep-ph/0011336 [hep-ph] .
- [63] C. W. Bauer and I. W. Stewart, *Phys.Lett.* **B516**, 134 (2001), arXiv:hep-ph/0107001 [hep-ph] .
- [64] C. W. Bauer, D. Pirjol, and I. W. Stewart, *Phys.Rev.* **D65**, 054022 (2002), arXiv:hep-ph/0109045 [hep-ph] .
- [65] M. Beneke, A. Chapovsky, M. Diehl, and T. Feldmann, *Nucl.Phys.* **B643**, 431 (2002), arXiv:hep-ph/0206152 [hep-ph] .
- [66] M. Beneke and T. Feldmann, *Phys.Lett.* **B553**, 267 (2003), arXiv:hep-ph/0211358 [hep-ph] .
- [67] I. W. Stewart, F. J. Tackmann, and W. J. Waalewijn, *Phys.Rev.* **D81**, 094035 (2010), arXiv:0910.0467 [hep-ph] .
- [68] I. W. Stewart, F. J. Tackmann, and W. J. Waalewijn, *JHEP* **1009**, 005 (2010), arXiv:1002.2213 [hep-ph] .
- [69] T. Becher and M. Neubert, *Eur.Phys.J.* **C71**, 1665 (2011), arXiv:1007.4005 [hep-ph] .
- [70] A. Martin, W. Stirling, R. Thorne, and G. Watt, *Eur.Phys.J.* **C63**, 189 (2009), arXiv:0901.0002 [hep-ph] .
- [71] J. L. Rainbolt, T. Gunter, and M. Schmitt, (2014), arXiv:1410.8058 [hep-ex] .